

Quantitative Observation of Grain Boundary Carbon Segregation in Bake-hardening Steels

Jun TAKAHASHI*¹
Naoki MARUYAMA*²

Masaaki SUGIYAMA*¹

Abstract

For the quantitative analysis of grain boundary segregation elements in various types of steel materials, grain boundary observation techniques using a three-dimensional atom probe were constructed. This paper demonstrates the quantitative analysis of carbon atoms segregating on grain boundaries in ultra low carbon bake-hardening (BH) steel sheets. Since the segregation state depends on their boundary characteristics, the grain boundaries of specimens were characterized from Kikuchi pattern analysis before probing. The concentration and width of carbon segregation on large angle grain boundaries, which were the main boundaries of this material, were quantified to be about 2 at. % and 2 nm, respectively. From this result, the total amount of carbon atoms segregating on all grain boundaries was estimated to be about 2 wt. ppm (8 at. ppm). This value is very small compared to the intragranular solute carbon, and thus the contribution of the segregating carbon to bake hardenability is not so large.

1. Introduction

Examining the states of existence and behavior of alloying elements in steel that affect the properties of the material is very important for the design of steel materials. While the accuracy in the observation of the segregation of elements in steel has improved thanks to the advance of observation techniques such as transmission electron microscopy¹⁾, the three-dimensional atom probe (3D-AP) method is viewed as one of the most effective tools for further enhancing the space resolution and improving the detection limits of element measurement. However, while it is easy by the atom probe method to analyze the states of elements that are homogeneously distributed in steel, in order to analyze a local region by the method, it is necessary to prepare a specimen that includes the region in question, because the analyzed region is very small. For observing a crystal grain boundary of steel, in particular, it is necessary to prepare specimen of a needle shape with a grain boundary positioned at the tip portion²⁻⁵⁾.

This paper reports the quantitative observation of the segregation of carbon atoms at a grain boundary of a bake-hardening (BH) steel sheet as an application of the 3D-AP method, the establishment of a fundamental technique that enables grain boundary observation at a high success rate based on the method, and the problems related to the technique. There have been reports on the influence of grain boundary carbon segregation on the aging properties and bake-hardenableability of BH steel sheets⁶⁻⁹⁾, but a lot still remains unclear because of the difficulty in distinguishing the influence of the carbon segregation from other factors such as grain size. We reported herein quantified the carbon segregation at a specific grain boundary and estimated the total amount of carbon segregation at all grain boundaries using an ultra-low-carbon BH steel sheet as the sample.

2. Sample Steel

Table 1 shows the chemical composition (in wt. %) of the ultra-low-carbon BH steel sheet that the authors used for the test. The

*¹ Advanced Technology Research Laboratories

*² Steel Research Laboratories

Table 1 Chemical composition of sample steel (wt. %)

C	Si	Mn	P	N	sol.Al	Ti
0.0034	0.006	0.49	<0.002	0.0022	0.014	0.009

Table 2 Mechanical properties of sample steel

Grain size (mm)	Yield strength (MPa)	Tensile strength (MPa)	BH* (MPa)
15.2	211	326	81

* 2% prestrain → 170°C × 20min

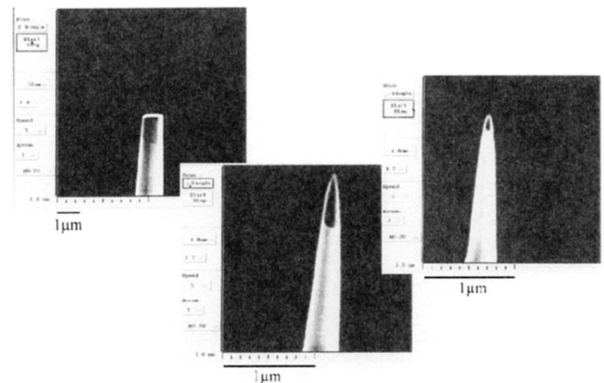
sample steel was hot rolled, then cold rolled at a reduction ratio of 80% into a sheet 0.8 mm in thickness on laboratory equipment, and then subjected to recrystallization annealing at 800°C for 60 s followed by cooling at a rate of 50°C/s, over-aging treatment at 350°C for 180 s and finally skin-pass rolling at a reduction ratio of 1%. Test pieces were cut out from the steel sheet thus prepared and subjected to tensile tests. Some of the test pieces underwent a pre-strain of 2%, aging treatment at 170°C for 20 min and then a second tensile test, and the amount of bake hardening (BH amount) was defined as the increment of the upper yield point. **Table 2** shows the mechanical properties and average grain size of the sample steel sheet. Since the C content was somewhat high at 34 ppm, the average BH amount was as high as above 80 MPa.

The specimens for the 3D-AP observation were prepared from square bars 0.25 mm × 0.25 mm in section that had been cut out from the center portion of the steel sheet before the skin-pass rolling.

3. Specimen Fabrication

In order to observe a grain boundary, it is necessary to prepare a needle-shaped AP specimen that includes a grain boundary; three such specimens were prepared for this experiment using a focused ion beam (FIB) system (FB2000A by Hitachi Ltd.)^{4,5,10}. A specimen formed into a needle shape by electrolytic polishing was set on the stage of the FIB, and fabricated using an ion beam that could be scanned in desired patterns so that a grain boundary was positioned at the tip portion. At first, the specimen was positioned in a large angle to the direction of the beam to locate a grain boundary with a scanning ion microscope (SIM), then, the portion above the grain boundary located was cut off with an ion beam. Since grains of different orientations show contrast under a SIM as a result of channeling effect, it is possible to identify a grain boundary. After cutting off the portion above the grain boundary, the specimen was set in parallel to the beam direction, and it was fabricated into a needle shape with an ion beam scanned in a ring pattern. In order to minimize the damage to the inside of the specimen caused by the beam irradiation, it was dismounted from the device without SIM observation from the side after the machining, and the position of the grain boundary was confirmed using a transmission electron microscope (TEM).

By repeating the above FIB fabrication and TEM observation one after the other, the specimen was produced so that the grain boundary was at 50 to 200 nm from the tip and the specimen diameter at the position of the boundary was as small as possible. A small tip portion was left beyond the boundary because it was necessary to prevent the damage caused by the beam from extending to the boundary; the portion damaged by the beam was removed by field evaporation before the 3D-AP measurement. The specimen diameter at the position of the boundary was made as small as possible because the

**Photo 1 FIB fabrication flow by SIM observation**

size of the portion determined the probing voltage and it was necessary to use as low a voltage as possible to minimize the damage to the specimen. **Photo 1** shows SIM observations of the machining processes to fabricate a needle-shaped specimen that includes a grain boundary at the tip portion.

4. Measurement of Misorientation Angle

It is desirable to discuss the distribution of atoms segregating at an observed grain boundary in consideration of the characteristics of the boundary. In view of this, before the 3D-AP measurement, the misorientation angle was determined⁵⁾ by measuring the Kikuchi patterns near the grain boundary at the tip using a TEM nano-probe. For precisely describing the characteristics of a boundary, it is necessary to determine the relative orientation of the two crystal grains that meet at the boundary and the orientation of the boundary itself¹⁾; in this experiment, the misorientation angle and rotation axis of each of the specimens were calculated.

Fig. 1 shows an example of the Kikuchi pattern analysis. Kikuchi bands can be indexed easily based on the width and orientation. Three poles were selected and an orientation matrix was calculated for each of the two crystal grains that met at the boundary. There are 24 different sets of coordinates in total, and 24 rotation angles are obtained through calculating the rotation matrices for the sets of coordinates; the smallest among them is the misorientation angle. In the example shown in Fig. 1, the misorientation angle ϕ was 47.7° and the rotation axis l was [-0.830, -0.306, -0.467], as shown in the table.

Photo 2 shows TEM bright-field images of the three specimens subjected to the grain boundary observation, and **Table 3** the misorientation angle and rotation axis of each of them calculated based on the Kikuchi pattern analysis. All the grain boundaries of the three specimens were high-angle boundaries. The same sample BH steel sheet was measured by the electron back scattering diffraction pattern (EBSP) method, and most of the grain boundaries were found to be high-angle boundaries having a misorientation angle of 30 to 60° and not to be coincidence boundaries. From this, the grain boundaries of the three specimens used for the present test were regarded to represent those of the sample steel sheet.

5. Test Results

5.1 Measurement results of 3D-AP

The unwanted portion at the tip of each of the specimens (including the portion damaged by the FIB machining) was removed by field evaporation, and the probing was commenced after confirming

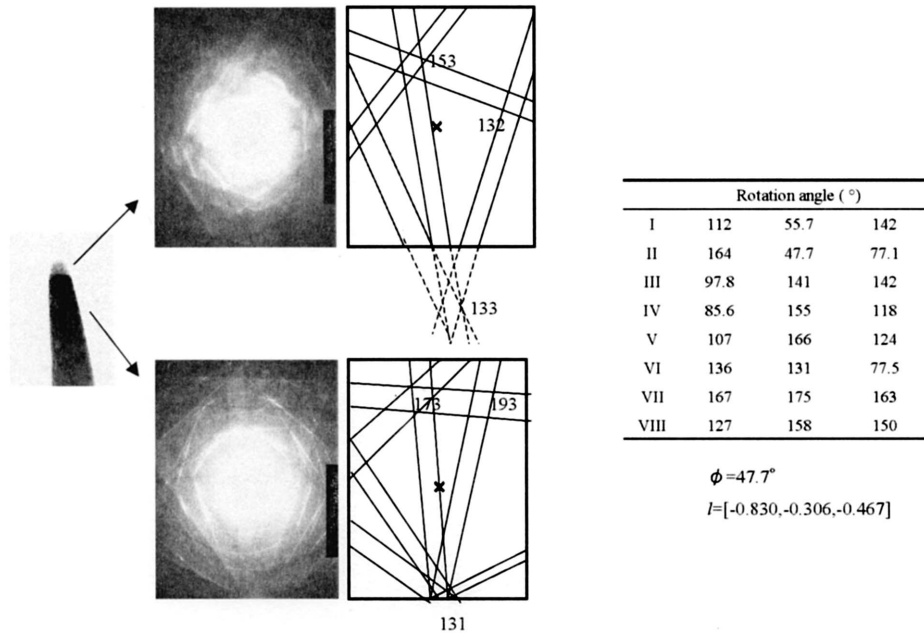


Fig. 1 Example of grain boundary characterization by Kikuchi pattern analysis

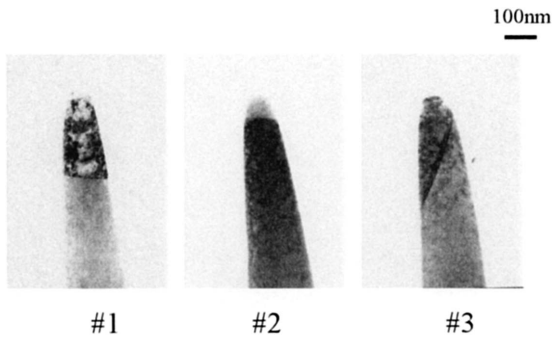


Photo 2 TEM bright field images of specimen tips including a grain boundary

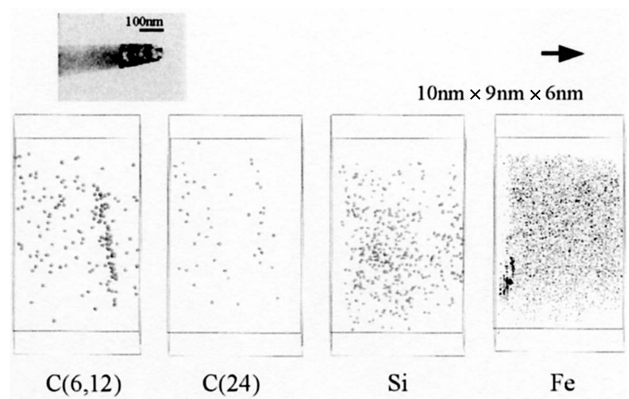


Fig. 2 3D elemental maps of specimen #1

Specimen	Misorientation angle (°)	Rotation axis
#1	47.0	$[-0.863, 0.473, -0.178]$
#2	47.7	$[-0.830, -0.306, -0.467]$
#3	53.4	$[0.016, 0.071, -0.704]$

the grain boundary in an FIM image. The measurement temperature was set at 65 to 75 K, and Ne gas was introduced at 1×10^{-8} Torr or less⁵⁾ in order to lower the field evaporation voltage and prevent the tip from rupturing.

Figs. 2 to 4 show elemental maps at the grain boundary portions that were obtained through reconstructing measurement data three-dimensionally. The arrows in the figures indicate the direction of probing, and TEM photographs of respective specimens are included in the figures in the same orientation as that of the maps. Carbon is detected, normally, as a C^{2+} ion having a mass-to-charge ratio of 6 and a C^+ ion having a mass-to-charge ratio of 12, and in a region

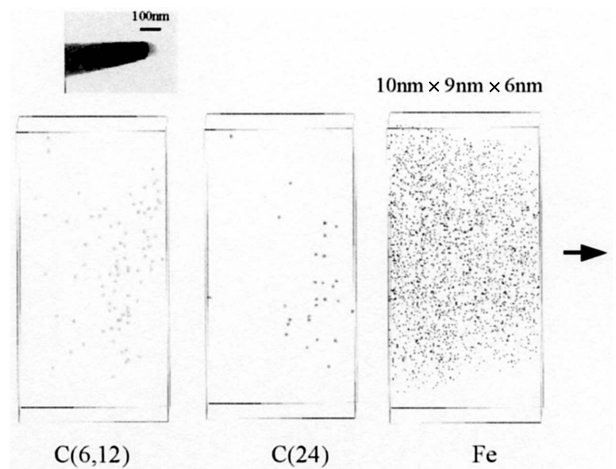


Fig. 3 3D elemental maps of specimen #2

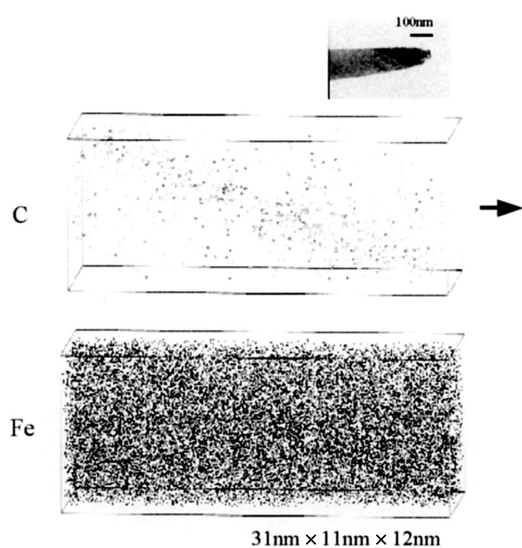


Fig. 4 3D elemental maps of specimen #3

where the segregation concentration of C is high, it is detected also as a C_2^+ compound ion having a mass-to-charge ratio of 24. These carbon ions are shown in the figures separately. Fig. 2 shows the probing result of a specimen having the grain boundary substantially perpendicular to the probing direction. One sees here C atoms segregate intensively at the boundary surface; on the other hand, Si is not found to segregate at the boundary. Fig. 3 shows the probing result of another specimen having the grain boundary substantially perpendicular to the probing direction. The data were obtained in a high vacuum without introducing Ne, and as a consequence, there was very little noise. Fig. 4 shows the probing result of a specimen having the grain boundary slanted in a large angle to its axis. One sees here C atoms (C^{2+} , C^2 and C_2^+) segregate intensively at the slanted boundary plane; on the other hand, Si, Mn and other alloying elements are not found to segregate at the boundary.

5.2 Element quantification

The authors quantitatively analyzed the state of C segregation based on the above results. In order to estimate the amount of grain boundary segregation, it is necessary to cut out a box in right angles to the boundary plane and calculate the concentration of a segregating element from a ladder diagram⁹⁾. Fig. 5 shows an example of the ladder diagram analysis of carbon segregation. The abscissa of the diagram represents the counting of all atoms in the box depth direction, and the ordinate the number of C atoms. The gradient represents the concentration of C atoms: a region where the gradient is steep corresponds to grain boundary segregation. From the figure, the segregation concentration of C atoms was estimated at 2.4 at. %, and the width of the segregation band at 0.86 nm. The amount of C in the portions other than the grain boundary was estimated at 0.23 at. %. However, this figure is 10 times or more the real concentration of solute C. While this difference is attributed to the misidentification of background noise as C atoms, since the estimated figure is less than one-tenth the concentration of the grain boundary C segregation, the difference does not affect the estimation of the segregation concentration.

Fig. 5 shows that, subtracting the amount of solute C and background noise, 85 atoms of C were detected at the grain boundary. Assuming that the ion detection ratio of the detector is 60%, the num-

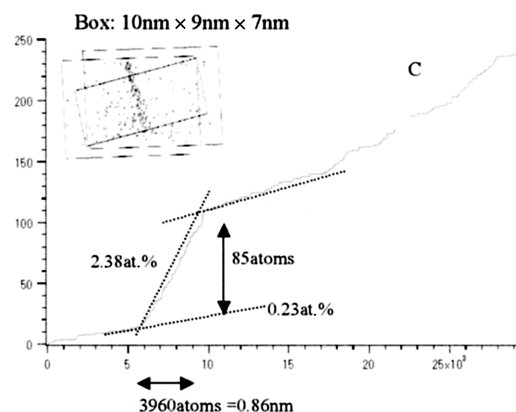


Fig. 5 Example of ladder diagram analysis

Table 4 Quantitative results of grain boundary carbon segregation

Specimen	Concentration (at. %)	Width (nm)	C-excess (at./nm ²)
#1	2.4	0.86	1.7
#2	2.4	1.26	2.5
#3	1.1	5.6	3.1

ber of C atoms segregating at the grain boundary area of the box is $85/0.6 = 142$. Because the grain boundary area of the box is given as the sectional area of the box, which is $84 \text{ nm}^2 (= 9.6 \text{ nm} \times 8.8 \text{ nm})$, the density of the C atoms segregating at a unit grain boundary area is $142/84 = 1.7 \text{ (atoms/nm}^2\text{)}$. This figure is defined as the "C-excess¹²⁾." Table 4 summarizes the results of the quantification of C segregation obtained through the present analysis.

From the above results, the average concentration of the C atoms segregating at the grain boundaries of the sample ultra-low-carbon BH steel sheet was estimated at approximately 2 at. %. This figure is more than 100 times the amount of C addition and more than 200 times that of solute C. The segregation concentration and the width of a segregation band varied somewhat from specimen to specimen. One of the possible reasons for the variation is that the boxes were not cut out exactly in right angles to the plane of the boundary. Therefore, use of the C-excess, which represents the increment of C per unit grain boundary area, is effective in quantitatively comparing the amounts of grain boundary carbon segregation. Another possible reason is that the shape of the specimen tip surface where the grain boundary exposes itself is not always ideal, and as a result, the adverse effect on the space resolution in the direction perpendicular to the probing direction (local magnification effect) becomes significant when the angle between the grain boundary and the probing direction is small^{5,13)}.

6. Estimation of Total Amount of Grain Boundary Carbon Segregation

The authors estimated the total amount of C atoms segregating at all grain boundaries based on the amount of the C segregation at a grain boundary obtained through this experiment. Letting the length of an edge of a cubic grain be D , and the width of grain boundary segregation be $W = 2a$, the boundary-to-volume ratio R_b is given as follows:

$$R_b = \frac{D^3 - (D - 2a)^3}{D^3} = 3(W/D) - 3(W/D)^2 + (W/D)^3 \quad (1)$$

Then, assuming that the average grain size D is approximately 15 μm and the grain boundary width W is 2 nm, the boundary-to-volume ratio R_b is 4.0×10^{-4} . Assuming, further, that the concentration of C atoms segregating at grain boundaries is 2 at. %, then, the total amount of grain boundary C segregation is given as:

$$2 \text{ at. \%} \times 4.0 \times 10^{-4} = 8.0 \text{ at. ppm} = 1.7 \text{ wt. ppm} \quad (2)$$

There have been few reports on the quantification of the total amount of grain boundary segregation directly from experiment, but according to a report that estimated the total amount of the grain boundary C segregation of an ultra-low-C steel sheet based on chemical analysis and internal friction, the estimated amount is approximately 6 wt. ppm¹⁴⁾. The value obtained through this experiment is less than a half of the reported value. On the other hand, some papers report that C and N atoms segregating at grain boundaries significantly contribute to the improvement of the BH and suppressed-aging properties of a steel sheet⁶⁻⁹⁾. However, judging from the fact that the value of approximately 2 wt. ppm of equation (2) is considerably smaller than the amount of solute C, which is estimated to be 10 to 20 wt. ppm, the direct influence of the grain boundary C segregation on BH properties by fixing dislocations inside crystal grains is considered to be small. What is more, the energy for trapping a C atom in a grain boundary is sufficiently larger than that at the temperature of bake hardening, 170°C, and it is therefore difficult to suppose that the atoms are freed from grain boundaries at the temperature.

Even in an estimation assuming a tetradecahedron (a truncated octahedron as a simple example) as a better approximation of crystal grain shape, the total amount of the grain boundary C segregation is larger than that in an estimation assuming a cube by approximately 10% only¹⁵⁾. Thus, the assumption of grain shape does not have a significant influence on the estimation of the total amount of grain boundary segregation. Judging from the facts such as that crystal grain size is widely varied in a real steel sheet, that grain shape is asymmetric, and that there is microscopically small unevenness on the surfaces of a crystal grain, the real amount of the total grain boundary carbon segregation is probably higher than the estimation of equation (2). However, even if the real value is twice the estimation as a result of the above factors, it will only be 4 wt. ppm or so, and the direct effects of the grain boundary C segregation on the BH properties ought to be limited.

7. Present Problems and Future Prospect

The authors added a small amount of Ne gas to reduce the damage to the needle-shaped specimens during the 3D-AP measurement. As a result, the level of background noise was higher in the present measurement compared with measurement under a high vacuum. Such a high noise level has adverse effects on the lower detection limits of microalloying elements. The ideal is to measure the elements under a high vacuum without introducing Ne gas, and for this end, appropriate measures will be required such as decreasing the diameter of a specimen yet further to reduce the risk of its being damaged.

As has been made clear through the present test, the technique of specimen preparation constitutes the key to the quantitative observation of a local region that has an influence on the properties of a whole steel material. For the purpose of sampling a specific grain boundary for future application of the quantitative observation technique, the authors tested the preparation of specimens using a microsampling system mounted on a FIB. **Photo 3** shows an ex-

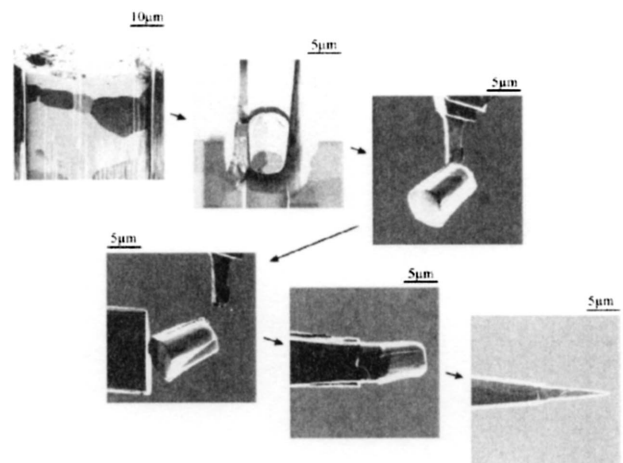


Photo 3 Application by FIB microsampling method

ample of the sampling of a specific grain boundary. A section surface of a steel material was observed with a FIB-SIM, a sample that included a grain boundary at a specific position was cut out in a cylindrical shape, fixed on a needle base by tungsten vapor deposition and machined into a needle shape using the FIB with a beam that could be scanned in desired patterns. The photomicrographs show that there is a grain boundary near the needle tip. While there still are many technical problems to solve, the development and application of the technology herein described will enable observation of very small local regions.

8. Closing

Applying the 3D-AP method, the authors quantified the amount of carbon segregating at a grain boundary of a bake-hardening steel sheet and estimated the amount of carbon segregating at all the grain boundaries. A technique for efficiently quantifying elements segregating at grain boundaries of steel was established and some problems of the technique were pointed out through this experiment. The authors expect innovative analysis techniques such as the one herein presented to be instrumental in clarifying phenomena in which grain boundary segregation elements are involved and to other technical breakthroughs.

Acknowledgement

For the present test, the authors were permitted to use the 3D-AP equipment (EC-TAP) of Metallic Nanostructure Group, Materials Engineering Laboratory of the National Institute for Materials Science (NIMS), for which they are much grateful. They also express their sincere gratitude to NIMS Fellow Dr. K. Hono, Dr. D. H. Ping and Dr. T. Okubo for fruitful discussion and advice.

References

- 1) Daita, K., Yanaka, T., Moriyama, K.: *Materia*. 39, 151 (2000)
- 2) Karlesson, L., Nolden, H.: *Acta Metall.* 36, 13 (1988)
- 3) Krakauer, B.W., Hu, J.G., Kuo, S.-M., Mallick, R.L., Seki, A., Seidman, D.W., Baker, J.P., Loyd, R.J.: *Rev. Sci. Instrum.* 61, 3390 (1990)
- 4) Seto, K., Larson, D.J., Warren, P.J., Smith, G.D.W.: *Scripta Mater.* 40, 1029 (1999)
- 5) Maruyama, N.: Ph.D. Thesis. Oxford University, 2001
- 6) Hanai, S., Takamoto, N., Tokunaga, Y., Mizuyama, Y.: *Tetsu-to-Hagané*. 68, 1169 (1982)
- 7) Ohsawa, K., Kinoshita, M., Nishimoto, A.: *Development of High-strength Steel Studies*. ISIJ, 1989, p.44

- 8) Yamazaki, Y., Imanaka, M., Morita M.: Japanese Unexamined Patent Publication. No. He7-300623
- 9) Kaneko, S., Shimizu, T.: Japanese Unexamined Patent Publication. No. He12-297350
- 10) Larson, D.J., Foord, D.T., Petford-Long, A.K., Anthony, T.C., Rozdilsky, I.M., Cerezo, A., Smith, G.D.W.: *Ultramicrosc.* 75, 147 (1998)
- 11) Ikuhara, Y., Yamamoto, T.: *Electron Microscopy.* 37, 51 (2002)
- 12) Hondros, E.D., Seah, M.P.: *Physical Metallurgy*, North Holland, Amsterdam, 1983, p.855
- 13) Miller, M.K., Smith, G.D.W.: *Atom Probe Microanalysis. Principles and Applications to Materials Problem*, Material Research Society, Pittsburgh, 1989
- 14) Yamazaki, Y., Okada, S., Sato, S., Kato, T.: *Physical Metallurgy of IF Steel.* ISIJ, 1993, p. 217
- 15) Cahn, J.W.: *Acta Metall.* 4, 13 (1956)